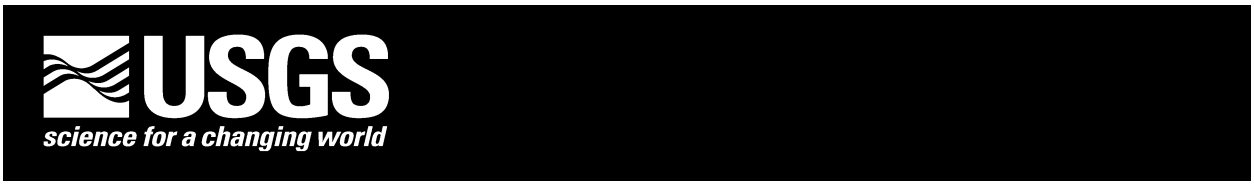


U.S. DEPARTMENT OF THE INTERIOR
U.S. GEOLOGICAL SURVEY

# Geophysical Constraints on the Virgin River Depression, Nevada, Utah, and Arizona

*by* V.E. Langenheim[1], J.M. Glen[1], R.C. Jachens[1], G.L. Dixon[2], T.C. Katzer[3], and R.L. Morin[1]

Open-File Report 00-407

2000



**U.S. DEPARTMENT OF THE INTERIOR**
**U.S. GEOLOGICAL SURVEY**

[1]Menlo Park, California
[2]Las Vegas, Nevada
[3]Cordilleran Hydrology, Inc., Reno, Nevada

## TABLE OF CONTENTS



FIGURES



TABLES

ABSTRACT

Gravity and aeromagnetic data provide insights into the subsurface lithology and structure of the Virgin River Depression (VRD) of Nevada, Utah, and Arizona. The gravity data indicate that the Quaternary and Tertiary sedimentary deposits hide a complex pre-Cenozoic surface. A north-northwest-trending basement ridge separates the Mesquite and Mormon basins, as evidenced by seismic-reflection, gravity, and aeromagnetic data. The Mesquite basin is very deep, reaching depths of 8-10 km. The Mormon basin reaches thicknesses of 5 km. Its northern margin is very steep and may be characterized by right steps, although this interpretation could change with additional gravity stations. Most of the young (Quaternary), small-displacement faults trend within 10° of due north and occur within the deeper parts of the Mesquite basin north of the Virgin River. South of the Virgin River, only a few, young, small-displacement faults are mapped; the trend of these faults is more northeasterly and parallels the basement topography and is distinct from that of the faults to the north. The Virgin River appears to follow the margin of the basin as it emerges from the plateau.

The high-resolution aeromagnetic data outline the extent of shallow volcanic rocks in the Mesquite basin. The north-northwest alignment of volcanic rocks east of Toquop Wash appear to be structurally controlled because of faults imaged on seismic-reflection profiles and because the alignment is nearly perpendicular to the direction of Cenozoic extension. More buried volcanics likely exist to the north and east of the high-resolution aeromagnetic survey. Broader aeromagnetic anomalies beneath pre-Cenozoic basement in the Mormon Mountains and Tule Springs Hills reflect either Precambrian basement or Tertiary intrusions. These rocks are probably barriers to ground-water flow, except where fractured.

## INTRODUCTION

The U.S. Geological Survey collected gravity and aeromagnetic data in support of hydrogeologic framework studies of the Virgin River depression (VRD; fig. 1). An earlier report discussed a high-resolution aeromagnetic survey (Jachens and others, 1998); this report adds to their analysis and incorporates constraints on basin structure from gravity data. Nearly 950 gravity stations were collected regionally and along several traverses within the basin. The gravity data were inverted for thickness of alluvial deposits using a method developed by Jachens and Moring (1990). Gravity stations were also collected outside the Virgin River Valley to provide control on basement and to provide a suitable extension of the gravity field for the depth-to-basement calculations. Several different models were created to provide limits on the configuration of the ground-water basin and locate faults within the basin. Aeromagnetic data were used to infer the subsurface extent of Tertiary volcanic rocks and relatively shallow (approximately less than 5 km or 3 mi) Precambrian crystalline basement rocks that may control the movement of groundwater.

## GEOLOGIC SETTING

The lower Virgin River Valley is a large alluvial basin bisected by the Virgin River and surrounded by the Beaver Dam Mountains on the east, the Virgin Mountains on the south, the Mormon Mountains to the west, and the Tule Springs Hills on the north (fig. 1). These ranges expose rocks ranging in age from Precambrian crystalline basement rocks to Mesozoic continental sedimentary deposits (fig. 2). The Paleozoic sequence consists of a mostly carbonate section, which lies between Cambrian and Permian clastic deposits; the Mesozoic section consists of continental and marine deposits of siltstone, sandstone, limestone, gypsum, conglomerate, and shale (Tschanz and Pampeyan, 1970; Longwell and others, 1965). These rocks were affected by the Sevier orogeny, an episode of Cretaceous and Tertiary decollement and basement-involved thrusting. Cretaceous synorogenic rocks were eroded from emerging thrust highlands and deposited in front of the advancing thrust sheets. The youngest pre-orogenic strata for most of the study area consist of the red Jurassic Aztec sandstone. In general, of the various bedrock units,

only the Paleozoic carbonate units have potential for transmitting large quantities of water (Winograd and Thordarson, 1975; Dettinger, 1989; McKee, 1997). The rest of the pre-Cenozoic sequence is well-consolidated and impermeable and tends to act as a barrier to ground water movement.

The Cenozoic sequence consists of two major unconformity-bounded syntectonic packages, the lacustrine and fluvial Horse Spring-Cottonwood Wash and the Muddy Creek sections. The Horse Spring-Cottonwood Wash sequence is composed of late Oligocene to Miocene conglomerate, shale, sandstone, siltstone, limestone, evaporites, and volcanic rocks (Longwell and others, 1965; Bohannon, 1984). This package unconformably overlaps Cretaceous and older rocks throughout the study area. Above the Horse Spring-Cottonwood Wash package are the sandstone, siltstone, conglomerate, evaporites, and basalt flows of the Miocene to Quaternary Muddy Creek Formation. Both of these Cenozoic sedimentary packages reflect the latest tectonic episode of the region by exhibiting large changes in thickness across basin-bounding normal faults according to seismic-reflection data (Bohannon and others, 1993; Carpenter and Carpenter, 1994).

The Muddy Creek Formation, extensively exposed throughout the VRD, has great variability in rock type from region to region. In the Mesquite basin, Williams (1996) described the unit in several facies: basal conglomerate, conglomerate bed of Toquop Wash, fine-medium-grained siltstone and claystone, and upper conglomerate facies. The variability of the unit probably accounts for its importance as a producing aquifer, especially when faulted (Dixon and Katzer, 2000). Both the Muddy Creek Formation and some of the Mesozoic formations contain gypsum, which is water-soluble and introduces sulfates into the ground-water system, causing very poor water quality. Some of the wells in the Mesquite basin have high concentrations of salts, which can be traced directly to ground water encountering gypsum from the Mesozoic and Tertiary sections (Dixon and Katzer, 2000).

Most of the extension occurred before the deposition of the Muddy Creek Formation (Bohannon and others, 1993), although seismic-reflection data do show some faults extending up into the Muddy Creek deposits. Numerous small-displacement faults offset Muddy Creek and younger alluvial deposits in the eastern part of the VRD (fig. 2; Billingsley and Bohannon, 1995; Billingsley, 1995; Williams, 1996, Dixon and Katzer, 2000). Muddy Creek deposits are tilted as much as $10^0$-$20^0$ towards the Beaver Dam Mountains (Hintze, 1986) and locally as much as $45^0$ near Mesquite (Williams, 1996). The offset of Quaternary deposits is as great as 36 m near the Arizona-Nevada border (Billingsley, 1995). Many of the small-displacement faults mapped north of the Virgin River coincide with and may have controlled the location of major washes (Dixon and Katzer, 2000).

## PREVIOUS GEOPHYSICAL WORK

Numerous seismic-reflection profiles were collected to support petroleum exploration efforts in the Virgin River Valley and vicinity. Several of these profiles are published in Bohannon and others (1993; blue lines on fig. 3) and Carpenter and Carpenter (1994; green lines on fig. 3). These profiles provide important independent constraints on the depth to pre-Cenozoic basement and indirect information on basin densities. The seismic-reflection profiles indicate that the VRD is underlain by two subbasins (fig. 2); the deeper Mesquite basin is separated from the Mormon basin by a north-trending ridge.

On a less regional scale, detailed seismic-refraction and electrical data were collected for a hydrological study of Beaver Dam Wash. Zohdy and others (1994) discusses 45 Schlumberger soundings along 5 profiles that cross Beaver Dam Wash and one longitudinal profile down the wash (triangles, fig. 3). They defined geoelectric basement as having resistivities of 70-1000 ohm-m, but found that geoelectric basement did not generally coincide with pre-Cenozoic basement. Higher resistivities often reflected the presence of caliche, unsaturated alluvium, or occasionally, better-quality ground water. Holmes and others (1997) also present the resistivity data of Zohdy and others (1994), but add 7 short (1 km or less) seismic-refraction profiles along parts of the resistivity profiles. Velocities ranged from 0.7 km/s (2,400 ft/s) for gravels to 5.2 km/s (17,200 ft/s) for “consolidated” rock.

Baer (1986) presented a preliminary analysis of the gravity and ground magnetic field of the area immediately north of the tri-state area. Griscom (1980) presented estimates to the tops of magnetic sources for the Virgin Mountains area. Another analysis of gravity and aeromagnetic data focused on the Mormon Mountains Wilderness Area (Shawe and others, 1988).

## DRILL-HOLE DATA AND PHYSICAL PROPERTIES

Although many water wells have been drilled in the Virgin River Valley, most are less than 200 m deep. As a result, only a few wells, which are restricted along the basin margins, provide information on depth to pre-Cenozoic rocks (Glancy and Van Denbergh, 1969; Holmes and others, 1997). An exception is the Mobil Virgin River No. 1-A oil well on Mormon Mesa, which penetrated Cretaceous and Jurassic clastic rocks at 2.0 km (6,702 ft) and Precambrian crystalline basement at a depth of 5.8 km (19,146 ft; Garside and others, 1988). Sonic velocities from the drill hole also provide valuable indirect information on densities (Bohannon and others, 1993).

Table 1 summarizes density measurements of hand-sized rock samples, all from the Virgin Mountains. Paleozoic sedimentary rocks have an average density of 2.68 g/cm$^3$ and Precambrian rocks have an average density of 2.78 g/cm$^3$. These values are consistent with densities from the Las Vegas and Lake Mead areas (Langenheim and others, 1998; Langenheim and others, 1999). The Paleozoic densities may be slightly too low, as the distribution of samples was somewhat skewed towards clastic lithologies. We did not measure any densities from the Mesozoic sedimentary section, but an average density of 2.50 g/cm$^3$ was obtained for Mesozoic rocks exposed in areas to the west and south.

Table 1. Densities and susceptibilities

| Number of Samples | Density Range (g/cm$^3$) | Average Density | Susceptibility Range ($10^{-3}$ cgs units) | Average Susceptibility |
|---|---|---|---|---|
| **Precambrian crystalline rocks** | | | | |
| 73 | 2.59-3.13 | 2.78±0.14 | 0.00-4.94 | 0.51±0.83 |
| **Paleozoic sedimentary rocks** | | | | |
| 8 | 2.58-2.84 | 2.69±0.09 | 0.00-0.10 | 0.00 |

No direct information is available on the density of the Cenozoic sedimentary deposits of the VRD. Indirect information comes from sonic velocities measured in the Mobil Virgin well and interval velocities from Carpenter and Carpenter (1994). Using the relationship of Gardner and others (1974) developed for sedimentary rocks,

$$\rho = 0.23 v^{0.25}$$

one can estimate the density, $\rho$ (g/cm$^3$), from the sonic velocity, v (ft/s). Sonic velocities measured on Cenozoic sedimentary rocks in the Mobil Virgin River 1A well are 2.1-3.0 km/s (7,000-10,000 ft/s) for the first second of two-way travel time (TWTT), increasing to 5.5 km/s (18,000 ft/s) at about 2 seconds TWTT (Bohannon and others, 1993). Interval velocities (Carpenter and Carpenter, 1994) are somewhat lower, but provide comparable densities at depths below 500-600 m (1,640-1,970 ft; table 2).

For comparison, densities calculated from measured porosities in one drill hole in Las Vegas Valley (Langenheim and Jachens, 1996) are between 2.08 and 2.30 g/cm$^3$ (unsaturated) and 2.31 and 2.45 g/cm$^3$ (saturated). These densities are similar to densities calculated from the velocity data (table 2).

Magnetic susceptibility data were collected on hand-sized samples. The Paleozoic sedimentary rocks are essentially non-magnetic (table 1). Susceptibilities of Precambrian crystalline rocks range from 0.0 to 4.94 x $10^{-3}$ cgs units, averaging 0.51 x $10^{-3}$ cgs units. Baer (1986) provides magnetic susceptibility estimates of 0.80-1.0 x $10^{-3}$ cgs for Precambrian crystalline rocks, 1.20-1.40 x $10^{-3}$ cgs units for Tertiary volcanic rocks, and 0.01-0.03 x $10^{-3}$ cgs units for Paleozoic to Cenozoic

sedimentary rocks, with valley fill slightly more magnetic. We do not have remanent magnetization measurements for the Cenozoic volcanic rocks, but we suspect that remanent magnetization could be a significant contribution to the total magnetization of some of the volcanic rocks exposed in the Grand Wash trough and Clover Mountains (fig. 1), and basaltic flows and dikes in the Muddy Creek Formation.

Table 2--Sonic velocities and corresponding densities

| Depth (in km)[1] | Average Velocity (km/s) | Density (g/cm$^3$) |
|---|---|---|
| (A) Mobil Virgin River 1A well from Bohannon and others (1993) | | |
| 0-0.5 | 2.1 | 2.11 |
| 0.5-1.3 | 2.3 | 2.15 |
| 1.3-2.1 | 3.3 | 2.35 |
| > 2.1 | 4.1 | 2.48 |
| (B) Interval velocities from Carpenter and Carpenter (1994) | | |
| 0-0.6 | 1.3 | 1.85 |
| 0.6-1.4 | 2.2 | 2.12 |
| 1.4-3.0 | 3.0 | 2.29 |
| >3.0 | 4.5 | 2.53 |

[1]Based on average velocity

## GRAVITY AND MAGNETIC DATA

Nearly 1,700 stations were used to create an isostatic gravity map of the region (fig. 4, Healey and others, 1981; Kane and others, 1979; Shawe and others, 1988; Cook and others, 1989). Gravity stations are non-uniformly distributed in the area (fig. 3). Station spacing is on average 2-3 stations per km$^2$, though the station spacing can be as low as 1 station per 10 km$^2$ in the mountainous regions and even within parts of the VRD.

New gravity data were collected with two LaCoste & Romberg gravity meters, G614 and G17C, during March, 1997; October 1999; and February and March 2000 (fig. 4) to supplement regional gravity coverage (Fig. 3) and provide detailed data over the ground water basin. The data were tied to a base station, MESC, established in front of the town hall in Mesquite. MESC has a value of 979593.62 mGal (IGSN71 datum) based on ties to CPA, a gravity base that is part of the Mt. Charleston calibration loop (Ponce and Oliver, 1981; observed gravity value of 979522.22 mGal).

Gravity data were reduced using the Geodetic Reference System of 1967 (International Union of Geodesy and Geophysics, 1971) and referenced to the International Gravity Standardization Net 1971 gravity datum (Morelli, 1974, p. 18). Gravity data were reduced to isostatic anomalies using a reduction density of 2.67 g/cm$^3$ and include earth-tide, instrument drift, free-air, Bouguer, latitude, curvature, and terrain corrections. An isostatic correction using a sea-level crustal thickness of 25 km (16 mi), a crustal density of 2.67 g/cm$^3$, and a mantle-crust density contrast of 0.40 g/cm$^3$ was applied to the gravity data to remove long-wavelength gravitational effect of isostatic compensation of the crust due to topographic loading. The resulting field is termed the isostatic gravity anomaly and reflects, to first order, density variations within the middle and upper crust (figs. 4a and b; Simpson and others, 1986).

Horizontal control on the gravity station locations was provided by hand-held Global Positioning System (GPS) units and Trimble Pathfinder GPS receivers and by 1:24,000-scale U.S. Geological Survey 7-1/2 minute series topographic maps. Regional station elevations were then extrapolated from stations' locations on the 1:24,000 topographic maps which have a contour interval of 6 m (20 feet). The uncertainty in the elevations of the stations is probably 3 m (10 ft) or less, with a corresponding error in the reduced gravity values of less than 0.6 mGal. Elevations

were obtained along the traverses using the Trimble GPS receivers and are accurate to less than 0.3 m (1 ft) with a corresponding error in the reduced gravity values of less than 0.06 mGal.

Terrain corrections were computed to a radial distance of 167 km (104 mi) and involved a 3-part process: (1) Hayford-Bowie zones A and B with an outer radius of 68 m (223 ft) were estimated in the field with the aid of tables and charts, (2) Hayford-Bowie zones C and D with an outer radius of 590 m (1,936 ft) were computed using a 30-m (100-ft) digital elevation model, and (3) terrain corrections from a distance of 0.59 km (1,936 ft) to 167 km (104 mi) were calculated using a digital elevation model and a procedure by Plouff (1977). Total terrain corrections for the stations collected for this study ranged from 0.06 to 17.1 mGal, averaging 1.5 mGal. If the error resulting from the terrain correction is considered to be 5 to 10% of the total terrain correction, the largest error expected for the data is 1.7 mGal. However, the error resulting from the terrain correction is small (less than 0.2 mGal) for most of the stations.

Aeromagnetic data (figs. 5a and b) consist of several regional surveys (Saltus and Ponce, 1988; Saltus and Snyder, 1986; Bankey and others, 1998) and a recently acquired high-resolution survey. The regional surveys were flown at various altitudes, directions, and flightline spacings (table 3). The regional data were adjusted to a common datum and then merged by smooth interpolation across survey boundaries. The recently acquired aeromagnetic survey (Jachens and others, 1998) was flown at a nominal height of 150 m (500 ft) above the ground. Flightlines were 400 m (0.25 mi) apart and oriented N70°W over the Virgin Valley and Tule Springs Hills and oriented N5$^0$W over the valley surrounding Meadow Valley Wash (see Jachens and others, 1998, for details of data collection and processing).

Table 3. Aeromagnetic survey specifications

| Name | Flightline spacing (mi) | Flightline direction | Altitude[1] (ft) | Reference |
|---|---|---|---|---|
| Virgin Mtns, NV | 0.5 | N-S | 1,000 AG | USGS (1979) |
| Caliente, NV | 1 | N-S | 9,000 B | USGS (1973) |
| Las Vegas, NV | 1 | E-W | 1,000 AG | USGS (1983) |
| Escalante UT | 3 | N-S | 400 AG | Geodata (1979) |
| Grand Canyon, AZ | 3 | E-W | 400 AG | LKB Resources, Inc, (1980) |

[1]B, barometric (constant altitude above sea level); AG, above ground

To help delineate trends and gradients in the gravity field, we used a computer algorithm to locate the maximum horizontal gravity gradient (Blakely and Simpson, 1986) (fig. 6a). Gradient maxima occur approximately over vertical or near-vertical contacts that separate rocks of contrasting densities; the horizontal displacement of a gradient maximum from the top edge of an offset horizontal layer is always less than or equal to the depth to the top of the source for moderate to steep dips (45° to vertical) (Grauch and Cordell, 1987). We also calculated magnetization boundaries (fig. 6b) in a similar way as described in Blakely and Simpson (1986), but using aeromagnetic data that were filtered to shift the anomalies over the sources (reduction to pole) and to emphasize shallow sources. Figure 6b reveals magnetization boundaries derived from the high-resolution aeromagnetic survey and regional coverage plotted on the filtered aeromagnetic data.

The Mesquite and Mormon basins are clearly defined in the regional gravity data as two pronounced gravity lows (amplitudes of 55 to 70 mGal with respect to surrounding mountain ranges) separated by a north-northwest-trending gravity ridge (fig. 4). The gravity lows are caused by low-density Muddy Creek and Horse Spring syntectonic sedimentary rocks resting on top of denser older rocks. The Grand Wash trough is also associated with a gravity low of approximately 40-50 mGal. Gravity highs with values exceeding +10-20 mGal occur over Paleozoic and Precambrian rocks exposed in the Virgin, Beaver Dam, and Mormon Mountains and the Colorado Plateau. Volcanic rocks and Mesozoic sedimentary rocks coincide generally with lower gravity values, on the order of -10 to -20 mGal, in the Clover and North Muddy Mountains.

The western margin of the Mesquite gravity low is marked by two steps in the gradient (marked "a" and "b"; fig. 4). The eastern gradient (east of Toquop Wash marked "b") parallels the 100-m (330 ft) and higher cliffs of Flat Top Mesa (fig. 1), composed of Muddy Creek sedimentary deposits capped with cemented gravels. A residual gravity low coincides with Flat Top Mesa, suggesting that part of the narrowing of the gravity gradient and accompanying low near Flat Top Mesa may reflect topography composed of materials of densities significantly lower than the density reduction of 2.67 g/cm$^3$. The maximum gravity effect of Flat Top Mesa calculated 3-dimensinally using a density contrast of –0.56 g/cm$^3$ (with respect to 2.67 g/cm$^3$) is about 4 mGal. This effect is important in that the basin inversion will attribute the gravity low over Flat Top Mesa to an increase in basin thickness, rather than low-density materials near the surface. Even after correcting for the effects of low-density materials composing Flat Top Mesa, a gravity gradient and relatively low gravity values still persist, suggesting that the basin is deep in this area.

Regional aeromagnetic data are dominated by strong magnetic highs over Precambrian crystalline rocks exposed in the Virgin, East Mormon and Beaver Dam Mountains (and presumably located at depth beneath the Mormon Mountains), and clusters of intense, relatively short-wavelength anomalies over Tertiary volcanic rocks exposed in the northern part of the study area (fig. 5). The broad magnetic highs over the Mormon Mountains coincide with gravity highs, and doming of the Cambrian Tapeats sandstone and the Mormon Peak detachment (Shawe and others, 1988). Shawe and others (1988) argued for the existence of a post-Tapeats (most likely Miocene) intrusion genetically related to the uplift and mineralization in overlying Paleozoic and younger strata. A broad magnetic high over the Tule Springs Hills is most likely caused by Precambrian basement at depth, though the northern part of the anomaly, which is more intense and shorter in wavelength, may reflect either shallower Precambrian basement or a Tertiary intrusion.

The north-northwest-trending broad magnetic high ("a"; fig. 5a) south of the magnetic highs over the East Mormon Mountains, is caused by the basement ridge that separates the Mesquite and Mormon basins seen in both gravity and seismic-reflection data. Another set of higher-frequency magnetic anomalies ("b", fig. 5a) east of Toquop Wash and north of the Virgin River approximately parallels the basement ridge. Bohannon and others (1993) suggested that the source of these anomalies along seismic-reflection profile I-81 (fig. 3) is shallow Precambrian basement. However, the gravity data indicate a low in this area and, thus, do not support a very shallow Precambrian basement ridge. The higher-resolution aeromagnetic data indicate that the source of these anomalies is buried less than 1 km deep and coincides with flat-lying reflections with tops at 800 and 500 m (2,620 and 1,640 ft; Jachens and others, 1998). Bohannon and others (1993) interpreted these bodies as gypsum. However, because gypsum is non-magnetic, a more likely cause for both the seismic reflections and the magnetic anomalies is volcanic rocks, possibly associated with basaltic flows in the Muddy Creek Formation (Jachens and others, 1998). The margins of this body are most likely controlled by faults seen in seismic-reflection data. Another shallow magnetic body ("c", fig. 5a) is evident in the southeast corner of the high-resolution aeromagnetic survey; in this case, the source is most likely reversely magnetized volcanic rocks and therefore, clearly cannot be composed of gypsum, as previously interpreted by Bohannon and others (1993).

Figure 6b shows magnetization boundaries calculated from the high-resolution aeromagnetic survey filtered to enhance shallow sources. Jachens and others (1998) interpreted the north-northwest grain of the anomalies south of the Virgin River as reflecting paleochannels, in part because the magnetic grain is at a high angle to mapped northeast-striking Quaternary faults in the area (fig. 6b). North of the Virgin River, several of the north-northwest-striking magnetization boundaries coincide with the major washes of the area, such as Beaver Dam and Toquop washes. These washes coincide with normal faults cutting the Muddy Creek Formation (Dixon and Katzer, 2000). However, many of the magnetization boundaries are not coincident with faults and most likely reflect various facies within the Muddy Creek Formation. In the Tule Desert, magnetization boundaries are characterized by both north-northeast and northwest trends. Jachens and others (1998) related the two sets of boundaries to the Tule Springs detachment fault and faults cutting Tertiary volcanic rocks to the north, respectively.

## DEPTH TO BASEMENT

We calculated the depth to bedrock, here defined to be pre-Cenozoic in age, beneath the Virgin River Valley and vicinity to define the shape of the Mesquite and Mormon subbasins and to determine the geometry of bounding and internal faults.

### Method

The method used in this study to estimate the thickness of Cenozoic rocks is an updated version of the iterative method developed by Jachens and Moring (1990) that can incorporate drill hole and other geophysical data (Bruce Chuchel, U.S. Geological Survey, written commun., 1996; Fig. 7). The method requires knowledge of the residual gravity field, exposed geology, and vertical density variation within the Cenozoic basin deposits. Data from drill holes that penetrate bedrock and geophysical data that provide constraints on the thickness of the basin fill are also input into the model and provide useful constraints to the method. The method separates the gravity field into two components, that which is caused by variations of density within the pre-Cenozoic bedrock and that which is caused by variations of thickness of the Cenozoic basin fill. To accomplish this process, the gravity data are separated into observations made on bedrock outcrops. The inversion is complicated by two factors: (1) bedrock gravity stations are influenced by the gravity anomaly caused by low-density deposits in nearby basins, and (2) the bedrock gravity field varies laterally because of density variations within the bedrock. The inversion presented here does not take into account lateral variations in the density distribution of the Cenozoic deposits.

To overcome these difficulties, a first approximation of the bedrock gravity field is determined by interpolating a smooth surface through all gravity values measured on bedrock outcrops. Bedrock gravity values are also calculated at locations where drill holes penetrated bedrock or seismic-reflection data constrain the bedrock surface, using the Cenozoic density-depth function (table 4). The basin gravity is then the difference between the observed gravity field on the original map and the first approximation of the bedrock gravity field and is used to calculate the first approximation of the thickness of Cenozoic deposits. The thickness is forced to zero where bedrock is exposed. This first approximation of the bedrock gravity is too low near the basin edges because of the effects of the nearby low-density deposits on the bedrock stations. The bedrock gravity station values are "corrected" for the effects of the low-density deposits (the effects are calculated directly from the first approximation of the thickness of the Cenozoic deposits) and a second approximation of the bedrock gravity field is made by interpolating a smooth surface through the corrected bedrock gravity observations. This iteration leads to an improved estimate of the basin gravity field, an improved depth to bedrock and a new correction to the bedrock gravity values. This procedure is repeated until successive iterations produce no significant changes in the bedrock gravity field.

Table 4. Density-depth functions

| Depth Range (m) | Density contrast ($g/cm^3$) ( Virgin well) | Depth Range (m) | Density contrast ($g/cm^3$) Based on Carpenter and Carpenter (1994) velocities |
|---|---|---|---|
| 0-500 | -0.56 | 0-600 | -0.82 |
| 500-1200 | -0.52 | 600-1400 | -0.55 |
| 1200-2100 | -0.33 | 1400-3000 | -0.38 |
| >2100 | -0.20 | >3000 | -0.14 |

### Results

We created three basin models (fig. 8). Because little is known about densities of Cenozoic volcanic rocks, let alone, their vertical distribution, we assumed the same density-depth relationship for Cenozoic volcanic rocks. All models utilize bedrock gravity stations. The first model uses the density-depth function derived from sonic velocities shown in Bohannon and others (1993) without

well and seismic constraints; the second, Bohannon and others' function and well and seismic constraints and the third, well and seismic constraints, but using densities derived from Carpenter and Carpenter (1994; table 4). The gravity data were modified to remove the topographic effects of low-density material at Flat Top Mesa. The local gravity low caused by near-surface low-density materials leads to an over-estimate of the thickness of basin fill because the gravity low will be modeled by adding material at depth using a much lower density contrast that that of surficial materials.

The resulting basin models, regardless of whether well and seismic control is utilized, are remarkably similar, although they differ in the magnitude of thicknesses (fig. 8). The basin models predict maximum thickness of 9-10 km (approximately 6 mi) about 5-10 km northeast of the town of Mesquite. These estimates are consistent with the maximum thickness (greater than 7.6 km) seen on seismic-reflection profiles, CC-4 and CC-5 (fig. 4; Carpenter and Carpenter, 1994), although our location is displaced 5 km towards the lowest gravity values. The seismic-reflection profiles clearly indicate that the basin fill increases in thickness towards the mountain front away from the lowest gravity values. Either basement densities or basin fill densities must increase. Our preferred interpretation is that basin-fill densities increase towards the mountain front, most likely reflecting higher-density gravels and or landslide deposits. The Mormon basin reaches thicknesses of 5 km (3 mi), about 10 km north of Black Ridge. Many of the young, small-displacement faults occur within the deeper parts of the Mesquite basin north of the Virgin River. South of the Virgin River, only a few, young, small-displacement faults are mapped; the trend of these faults parallels the basement topography and is distinct from that of the faults to the north. The Virgin River appears to follow the margin of the basin as it emerges from the plateau.

Other alluvial basins in the region are generally shallow, with basin fill 1 km or less. An exception is the Grand Wash trough. The Grand Wash trough may be 2-3 km (1-2 mi) deep as well, but the inversion is hampered by a paucity of gravity stations in the basin (Fig. 3).

The alluvial basins north of the Virgin River depression, such as the Tule Desert basin, are generally less than 1-km deep and characterized by moderate to shallow sides. Jachens and others (1998) pointed out that the lack of a significant gravity low associated with these basins is consistent with detachment faulting and the broad, gentle north-northeast-striking aeromagnetic gradient northwest of the Tule Springs Hills could reflect the buried tip of the westward-dipping Tule Springs detachment fault.

The basement gravity field produced by the models (fig. 9), regardless of the model parameters, indicates high basement gravity values over the Virgin and Mormon Mountains where Precambrian crystalline rocks are exposed. Low basement gravity values coincide with exposures of Mesozoic sedimentary rocks (e.g. North Muddy Mountains). Low basement gravity values also occur north of the uplifts flanking the Virgin River depression, perhaps reflecting granitic plutons underlying Cenozoic volcanic rocks of the Clover Mountains. If Miocene plutonism is responsible for aeromagnetic highs over the Mormon Mountains (Shawe and others, 1988), these plutons are more mafic than the roots of the Cenozoic volcanic rocks to the north or very small in volume because of elevated basement gravity values over the Mormon Mountains.

Model C (using the Carpenter and Carpenter density-depth relationship) appears to overestimate the density contrasts and creates very high basement gravity values (as high as +36 mGal, all in the basin) relative to values over exposed basement. For this reason, we prefer model B, which shows a ridge in the basement gravity (constrained by several basement picks from seismic-reflection data) coinciding with the broad aeromagnetic high between the Mesquite and Mormon basins.

## CONCLUSIONS AND RECOMMENDATIONS

The complex pre-Cenozoic basement surface beneath the VRD indicates that the basin thickness can vary dramatically over short distances. Assuming that these abrupt changes in thickness mark faults, we have mapped buried faults beneath the VRD (fig. 10). The Mesquite basin, approximately rectangular in plan view, can be divided into two domains separated by the Virgin River. The domain north of the Virgin River is characterized by the deepest fill in the VRD. Quaternary faults appear to be concentrated within this domain, with strikes within $10^0$ to $20^0$

degrees of north. South of the Virgin River, the basin fill is less than 6-7 km (approximately 4 mi) thick. A east-northeast trending ridge in the basement surface separates these two basin domains. The margins of the ridge, in part, coincide with Quaternary faults and are roughly parallel to the inferred direction of Cenozoic extension ($S65^0W$; Wernicke and others, 1988).

The Mormon basin is not as deep as the Mesquite basin. It appears to be an east-tilted half-graben, as seen in seismic-reflection data (Bohannon and others, 1993). Its northern margin is very steep. Axen and others (1990) suggested that the basin margin coincided with the Moapa Peak shear zone and accommodated 10-15 km (6-9 mi) of right-lateral offset. The basin model suggests that this edge of the basin may be characterized by right steps, although this interpretation could change with additional gravity stations.

The high-resolution aeromagnetic data outline the extent of shallow volcanic rocks in the Mesquite basin (shown in light orange, fig. 10). The north-northwest alignment of volcanic rocks east of Toquop Wash appear to be structurally controlled because of faults imaged on seismic-reflection profiles (Bohannon and others, 1993) and because the alignment is nearly perpendicular to the direction of Cenozoic extension. More buried volcanics likely exist to the north and east of the high-resolution aeromagnetic survey. Broader aeromagnetic anomalies beneath pre-Cenozoic basement reflect either Precambrian basement or Tertiary intrusions, shown in pink on figure 10. These rocks are probably barriers to ground-water flow, except where fractured.

Additional drill-hole data and a better density-depth function would allow us to greatly refine the current models of the VRD basins. Because our models are constrained only by basement gravity stations and spatially limited well and seismic data, the basement gravity field over the VRD cannot resolve basement gravity anomalies that have wavelengths less than the spacing between basement outcrops with gravity observations and wells and seismic control points (as much as 10 km across the VRD). Drill-hole data, particularly those wells that provide depths to basement rocks, could greatly improve the resolution of the basement gravity field. Additional geophysical data, such as seismic reflection or refraction or electrical data, would also provide much needed, independent constraints on basin thickness. The density-depth function could be improved by borehole gravity surveys in existing boreholes and by calculating interval velocities along existing seismic-reflection data.

Figure 11 shows the density of gravity stations using a 2- by 2-km grid. Areas of relatively sparse gravity coverage of possible hydrologic interest are circled in magenta. The Beaver Dam Wash area north of 37° is an area that is poorly mapped geologically and geophysically. This area may be an important link for groundwater moving south into the VRD. Another area of interest is the location and geometry of the Moapa shear zone north of the Mormon Basin and the ridge between the Mormon and Mesquite basins.

## ACKNOWLEDGMENTS

We thank Michael Johnson and the Virgin Valley water district for financial and logistical support without which such a study would not been possible. We also acknowledge reviewing efforts by David Ponce (U.S. Geological Survey, Menlo Park, CA).

# REFERENCES


Axen G.J., Wernicke, B.P., Skelly, M.F., and Taylor, W.J., 1990, Mesozoic and Cenozoic tectonics of the Sevier thrust belt in the Virgin River Valley area, southern Nevada in Wernicke, B.P., ed., Basin and Range extensional tectonics at the latitude of Las Vegas, Nevada: Geological Society of America Memoir 176, p. 123-154.

Baer, J.L., 1986, Reconnaissance gravity and magnetic survey of the northern Mesquite basin, Nevada-Utah, in Griffen, D.T., and Phillips, W.R., eds., Thrusting and Extensional Structures and Mineralization in the Beaver Dam Mountains, Southwestern Utah: Utah Geological Association Publication 15, p. 109-118.

Bankey, Viki, Grauch, V.J.S., and Kucks, R.P., 1998, Aeromagnetic and Gravity Maps and Data: A Web Site for Distribution of Data (on-line version): U.S. Geological Survey Open-File-Report 98-761 (http: greenwood.cr.usgs.gov/pub/open-file-reports/ofr-98-0761).

Billingsley, G.H., 1995, Geologic Map of the Littlefield quadrangle, northern Mohave County, Arizona: U.S. Geological Survey Open-File Report 95-559, 15 p.

Billingsley, G.H., and Bohannon, R.C., 1995, Geologic map of the Elbow Canyon quadrangle, northern Mohave county, Arizona: U.S. Geological Survey Open-File Report 95-560, 16 p., scale 1:24,000.

Blakely, R.J., and Simpson, R.W., 1986, Approximating edges of source bodies from magnetic or gravity anomalies: Geophysics, v. 51, p. 1,494-1,498.

Bohannon, R.G., 1984, Nonmarine sedimentary rocks of Tertiary age in the Lake Mead region, southeastern Nevada and northwest Arizona: U.S. Geological Survey Professional Paper 1259, 72 p.

Bohannon, R.G., Grow, J.A., Miller, J., and Blank, H.R., Jr., 1993, Seismic stratigraphy and tectonic development of Virgin River depression and associated basins, southeastern Nevada and northwestern Arizona: Geological Society of American Bulletin v. 105, p. 501-520.

Carpenter, J.A., and Carpenter, D.G., 1994, Structural and Stratigraphic Relations in a Critical Part of the Mormon Mountains, Nevada, in Dobbs, S.W., and Taylor, W.J., eds., Nevada Petroleum Society 1994 Conference Volume II, (Book 1), p. 95-126.

Cook, R.L., Bankey, Viki, Mabey, D.R., and DePangher, Michael, 1989, Complete Bouguer gravity anomaly map of Utah: Utah Geological and Mineral Survey Map 122, scale 1:500,000.

Dettinger, M.D., 1989, Distribution of carbonate-rock aquifers in southern Nevada and the potential for their development, summary of findings, 1985-88: Program for the Study and Testing of Carbonate-Rock Aquifers in Eastern and Southern Nevada, Summary Report No. 1, U.S. Geological Survey, Desert Research Institute, and University of Nevada.

Dixon, G.L., and Katzer, T.C., in press, Geology and hydrology of the lower Virgin River Valley in Nevada, Arizona, and Utah: Report for the Virgin Valley water district.

Dohrenwend, J.C., Schell, B.A., Menges, C.M., Moring, B.C., and McKittrick, M.A., 1996, Reconnaissance photogeologic map of young (Quaternary and late Tertiary) faults in Nevada: Nevada Bureau of Mines and Geology Open-File Report 96-2.

Gardner, G.H., Gardner, L.W., and Gregory, A.R., 1974, Formation velocity and density: the diagnostic basis for stratigraphic traps: Geophysics, v. 39, p. 770-780.

Garside, L.J., Hess, R.H., Fleming, K.L., and Weimer, B.S., 1988, Oil and gas developments in Nevada: Nevada Bureau of Mines and Geology Bulletin 104, 136 p.

Geodata, International, Inc., 1979, Aerial gamma ray and magnetic survey, Escalante national topographic map, Arizona and Utah: U.S. Department of Energy Report GJBX-15(880), scale 1:500,000.

Glancy, P. A., and Van Denburgh, A. S., 1969, Water-resources appraisal of the lower Virgin River Valley area, Nevada, Arizona, and Utah: Nevada Department of Conservation and Natural Resources, Water Resources Reconnaissance Series Report 51, 87 p.

Grauch, V.J.S., and Cordell, Lindrith, 1987, Limitations of determining density or magnetic boundaries from the horizontal gradient of gravity or pseudogravity data: Geophysics, v. 52, no. 1, p. 118-121.
Griscom, Andrew, 1980, Maps showing aeromagnetic survey and interpretation of the Virgin Mountains instant study area, Clark County, Nevada: U.S. Geological Survey Miscellaneous Field Studies Map MF-1204-C, scale 1:62,500.
Healey, D.L., Snyder, D.B., Wahl, R.R., and Currey, F.E., 1981, Bouguer gravity map of Nevada: Caliente Sheet: Nevada Bureau of Mines and Geology Map 70, scale 1:250,000.
Hintze, L.F., 1986, Stratigraphy and Structure of the Beaver Dam Mountains, Southwestern Utah, in Griffen, D.T., and Phillips, R.J., eds., Thrusting and Extensional Structures and Mineralization in the Beaver Dam Mountains, southwestern Utah: Utah Geological Association Publication 15, p. 1-36.
Holmes, W.F., Pyper, G.E., Gates, J.S., Schaefer, D.H., and Waddell, K.M., 1997, Hydrology and water quality of the Beaver Dam Wash area, Washington county, Utah, Lincoln County, Nevada, and Mohave County, Arizona: U.S. Geological Survey Water Resources Investigations Report 97-4193, 71 p.
International Union of Geodesy and Geophysics, 1971, Geodetic Reference System 1967: International Association of Geodesy Special Publication no. 3, 116 p.
Jachens, R.C., and Moring, B.C., 1990, Maps of the thickness of Cenozoic deposits and the isostatic residual gravity over basement for Nevada: U.S. Geological Survey Open-File Report 90-404, 15 p., 2 plates.
Jachens, R.C., Dixon, G.L., Langenheim, V.E., and Morin, R., 1998, Interpretation of an aeromagnetic survey over part of Virgin Valley, Tule Desert, and the valley surrounding Meadow Valley wash, southeastern Nevada: U.S. Geological Survey Open-File Report 98-804 16 p.
Kane, M.F., Healey, D.L., Peterson, D.L., Kaufmann, H.E., and Reidy, D., 1979, Bouguer gravity map of Nevada—Las Vegas sheet: Nevada Bureau of Mines and Geology Map 61, scale 1:250,000.
Langenheim V.E., Davidson, J.G., Anderson, M.L., and Blank, H.R., Jr., 1999, Principal facts for gravity stations and physical property measurements in the Lake Mead 30' by 60' quadrangle, Nevada and Arizona: U.S. Geological Survey Open-File Report 99-435, (http://geopubs.wr.usgs.gov/open-file/of99-435).
Langenheim, V.E., Grow, John, Miller, John, Davidson, J.D., and Robison, E., 1998, Thickness of Cenozoic deposits and location and geometry of the Las Vegas Valley Shear Zone, Nevada, based on gravity, seismic-reflection, and aeromagnetic data: U.S. Geological Survey Open-File Report 98-576, 32 p.
Langenheim, V.E., and Jachens, R.C., 1996, Thickness of Cenozoic deposits and groundwater storage capacity of the westernmost part of the Las Vegas Valley, inferred from gravity data: U.S. Geological Survey Open-File Report 96-259, 29 p.
LKB Resources, Inc., 1980, NURE aerial gamma-ray and magnetic reconnaissance survey, Colorado-Arizona area, Grand Canyon NJ 12-10 quadrangle, vol. II: U.S. Department of Energy Report GJBX-35(80), 96 p.
Longwell, C.R., Pampeyan, E.H., Bowyer, Ben, and Roberts, R.J., 1965, Geology and mineral deposits of Clark County, Nevada: Nevada Bureau of Mines and Geology Bulletin 62, 218 p.
McKee, E.H., 1997, Evaluation of geologic structure guiding ground water flow south and west of Frenchman Flat, Nevada Test Site: U.S. Geological Survey Open-File Report 97–734, 26 p.
Moore, R.T., 1972, Geology of the Virgin and Beaver Dam Mountains, Arizona: Arizona Bureau of Mines Bulletin 186, 65 p.
Morelli, Carlo, 1974, The International Gravity Standardization Net, 1971: International Association of Geodesy Special Publication no. 4, 194 p.
Plouff, Donald, 1977, Preliminary documentation for a FORTRAN program to compute gravity terrain corrections based on topography digitized on a geographic grid: U.S. Geological Survey Open-File Report 77-535, 45 p.
Ponce, D.A., and Oliver, H.W., 1981, Charleston Peak gravity calibration loop, Nevada: U.S. Geological Survey Open-File Report 81-985, 20 p.

Saltus, R.W., and Ponce, D.A., 1988, Aeromagnetic map of Nevada—Las Vegas sheet: Nevada Bureau of Mines and Geology Map 95, scale 1:250,000.
Saltus, R.W., and Snyder, D.B., 1986, Aeromagnetic map of Nevada--Caliente sheet: Nevada Bureau of Mines and Geology Map 89, scale 1:250,000.
Shawe, D.R., Blank, H.R., Jr., Wernicke, B.P., Axen, G.J., Barton, H.N., Day, G.W., and Rains, R.L., 1988, Mineral resources of the Mormon Mountains wilderness study area, Lincoln county, Nevada: U.S. Geological Survey Bulletin 1729, p. B1-B18.
Simpson, R.W., Jachens, R.C., Blakely, R.J., and Saltus, R.W., 1986, A new isostatic residual gravity map of the conterminous United States with a discussion on the significance of isostatic residual anomalies: Journal of Geophysical Research, v. 91, p. 8,348-8,372.
Snyder, D.B., Wahl, R.R., and Currey, F.E., Bouguer gravity map of Nevada—Caliente sheet: Nevada Bureau of Mines and Geology Map 70, scale 1:250,000.
Tschanz, C.M., and Pampeyan, E.H., 1970, Geology and Mineral Deposits of Lincoln County, Nevada: Nevada Bureau of Mines and Geology Bulletin 73, 188 p.
U.S. Geological Survey, 1973, Aeromagnetic map of the southeastern Lund and eastern half of the Caliente $1^0$ by $2^0$ degree quadrangles, Nevada: U.S. Geological Survey Open-FIle Report 73-298.
U.S. Geological Survey, 1979, Aeromagnetic map of the Virgin Mountains area, Nevada: U.S. Geological Survey Open-File Report 79-1235, scale 1:62,500.
U.S. Geological Survey, 1983, Aeromagnetic map of part of the Las Vegas $1^0$ by $2^0$ quadrangle, Nevada: U.S. Geological Survey Open-File Report 83-729, scale 1:250,000.
Wernicke, B.P., Axen, G.J., and Snow, J.K., 1988, Basin and Range extensional tectonics at the latitude of Las Vegas, Nevada: Geological Society of America Bulletin, V. 100, No. 11, p. 1738-1757.
Williams, V.S., 1996, Geology of the Mesquite Quadrangle, Clark County, Nevada: U.S. Geological Survey Open-File Report 96-676, (http://ncgmp.cr.usgs.gov/ncgmp/lvuc/mesquite/mesquite.htm).
Williams, V.S., Bohnannon, R.G., and Hoover, D.L., 1997, Geologic map of the Riverside Quadrangle, Clark County, Nevada: U.S. Geological Survey Geologic Quadrangle Map GQ-1770, scale 1:24,000.
Winograd, I.J., and Thordarson, W., 1975, Hydrogeologic and hydrochemical framework, south-central Great Basin, Nevada-California, with special reference to the Nevada Test Site: U.S. Geological Survey Professional Paper 712–C, 126 p.
Zohdy, A.A.R., Bisdorf, R.J., and Gates, J.S., 1994, A direct-current resisitivity survey of the Beaver Dam Wash drainage in southwest Utah, southeast Nevada, and northwest Arizona: U.S. Geological Survey Open-File Report 94-676, 87 p.

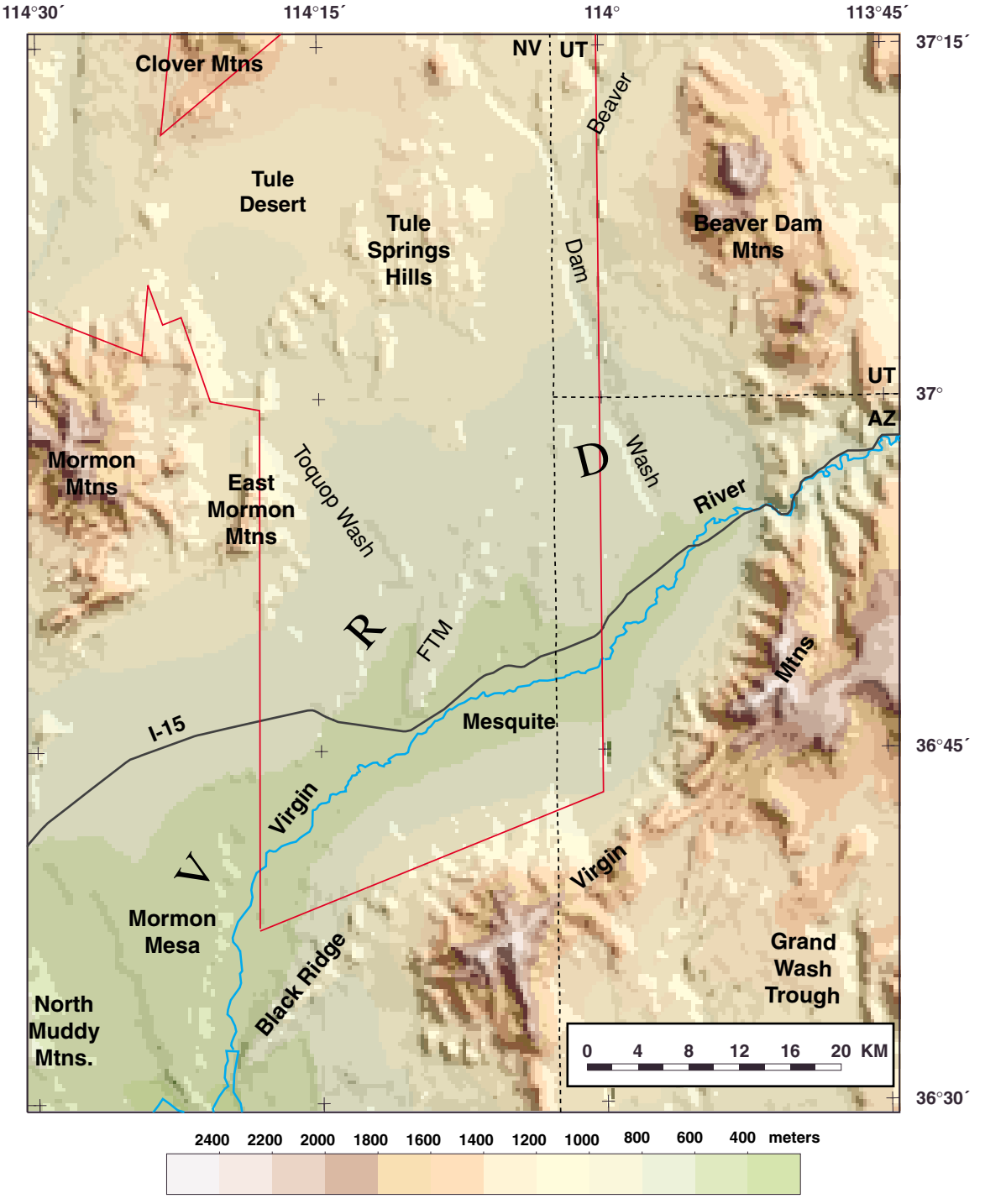


Figure 1. Shaded-relief topographic map of the Virgin River depression (VRD). High-resolution aeromagnetic survey (Jachens and others, 1998) outlined in red. FTM, Flat Top Mesa.

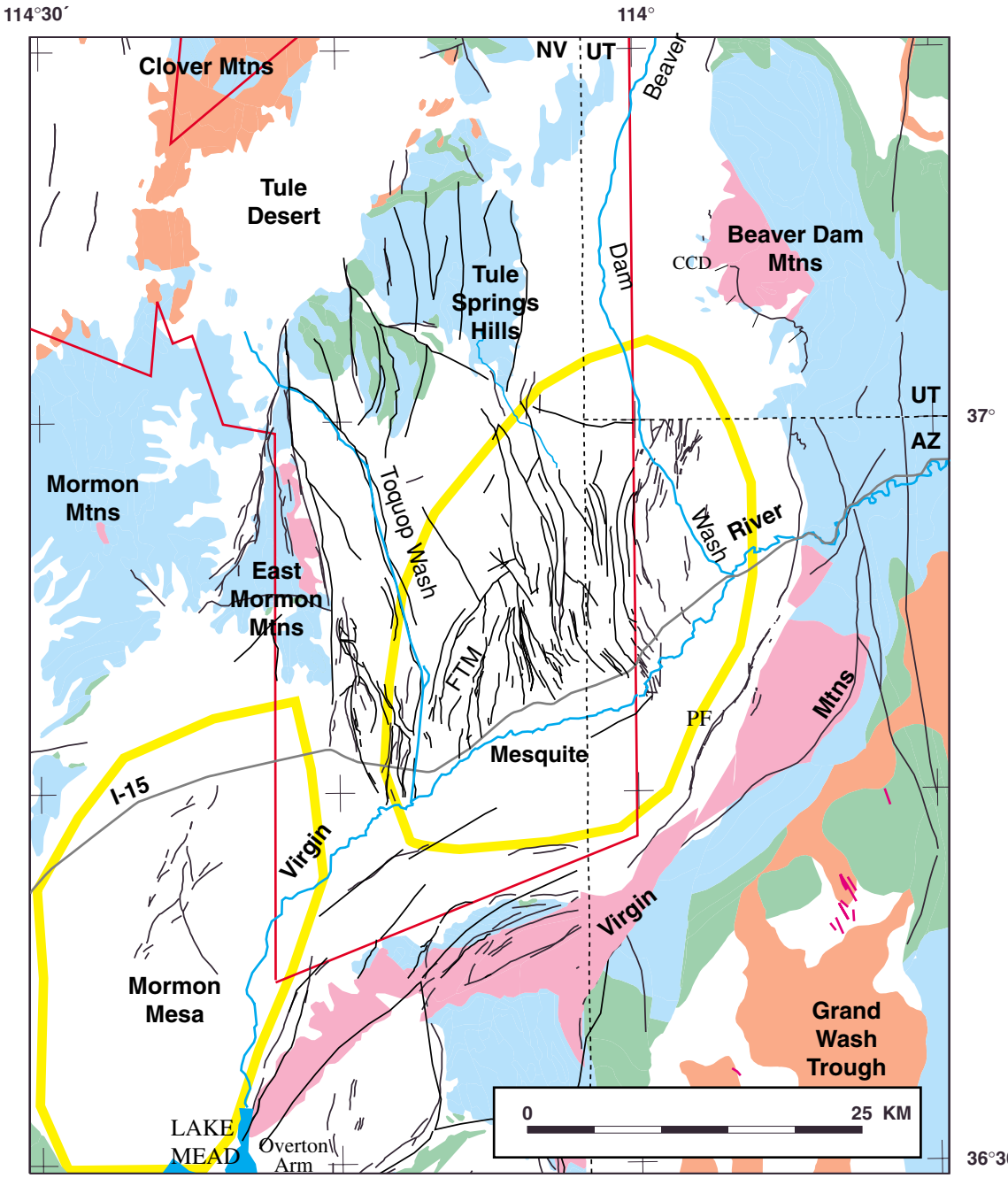


Figure 2. Simplified geologic map of the study area. Pink, Precambrian rocks; pale blue, Paleozoic rocks; green, Mesozoic rocks; light brown, Tertiary volcanic rocks; White, Quaternary and Tertiary sedimentary deposits. Magenta lines in Grand Wash Trough are Tertiary basaltic mapped dikes (Moore, 1972). Fault locations (in black) from Billingsley (1995), Billingsley and Bohannon (1995), Williams and others (1997), Dixon and Katzer (in press), Dohrenwend and others (1996), and Hintze (1986). Detailed fault locations in the basin do not extend into Utah. CCD, Castle Cliff detachment fault. PF, Piedmont fault. Thick yellow lines outline approximate extent of the Mesquite and Mormon basins.

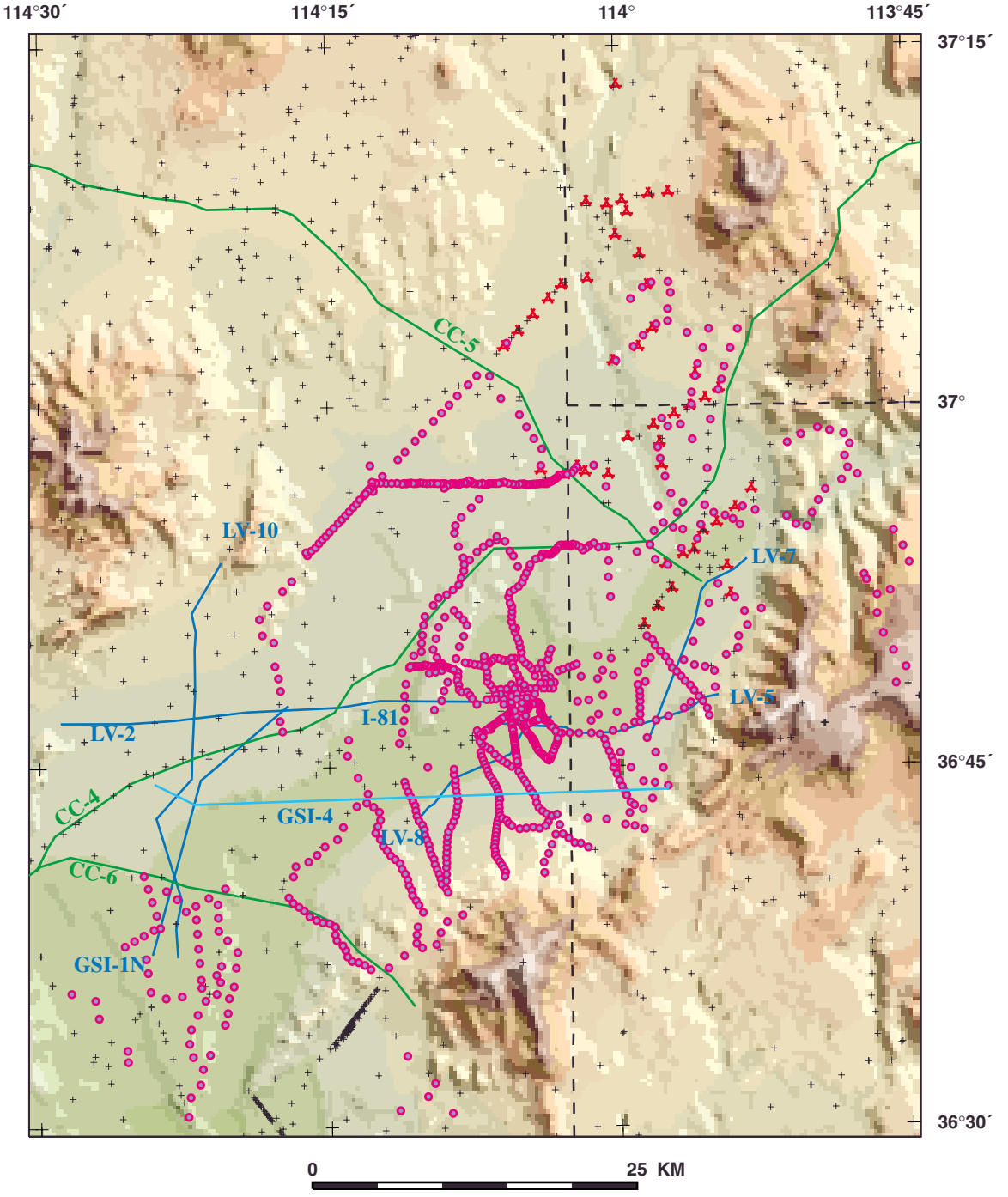


Figure 3. Geophysical data locations on shaded-relief topographic map (see Figure 1). New U.S. Geological Survey gravity stations shown in pink circles, older stations shown as black crosses. Red triangles are electrical sounding locations (Zohdy and others, 1994). Blue lines are seismic-reflection profiles discussed in Bohannon and others (1993) and green lines are seismic-reflection profiles shown in Carpenter and Carpenter (1994).

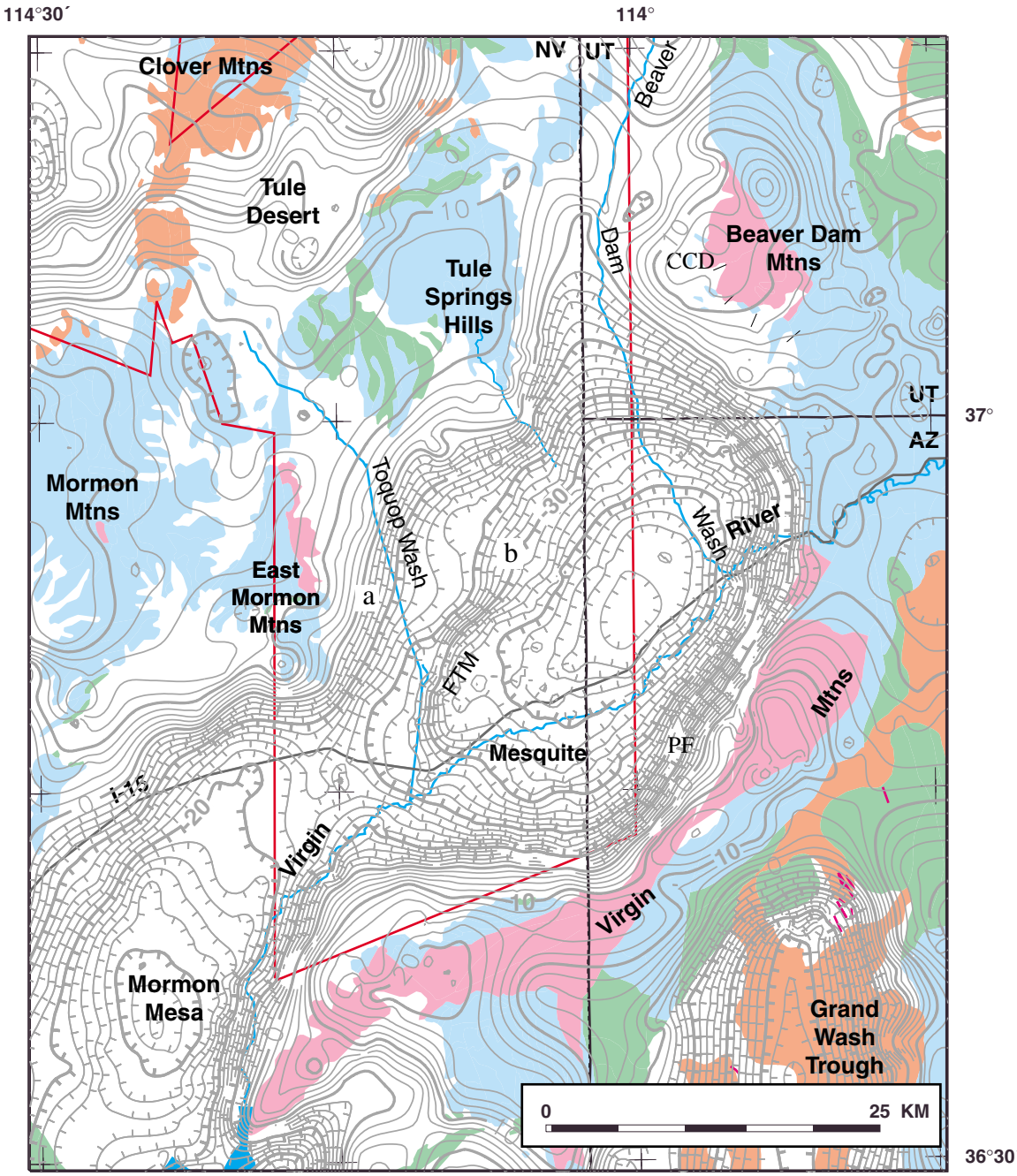


Figure 4a. Isostatic gravity contours on simplified geologic map. Contour interval, 2 mGal. See figure 2 for explanation of geology. "a" and "b" are steps in gravity gradient marking the western margin of the Mesquite basin.

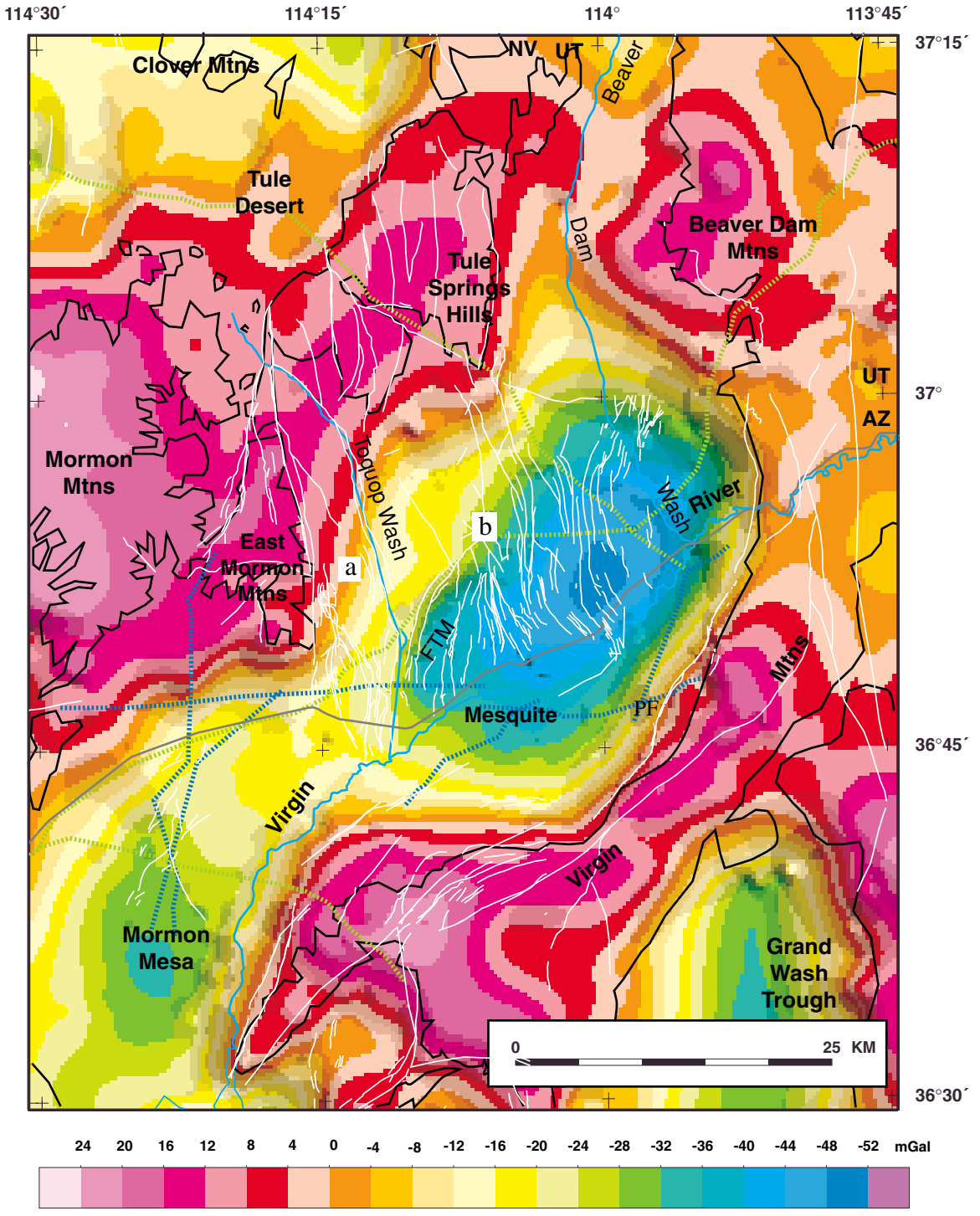


Figure 4b. Color version of isostatic gravity. Contour interval, 4 mGal. Green and blue lines are seismic-reflection profiles of Carpenter and Carpenter (1994) and Bohannon and others (1993), respectively; white lines, faults from figure 2. Black lines show extent of pre-Cenozoic basement.

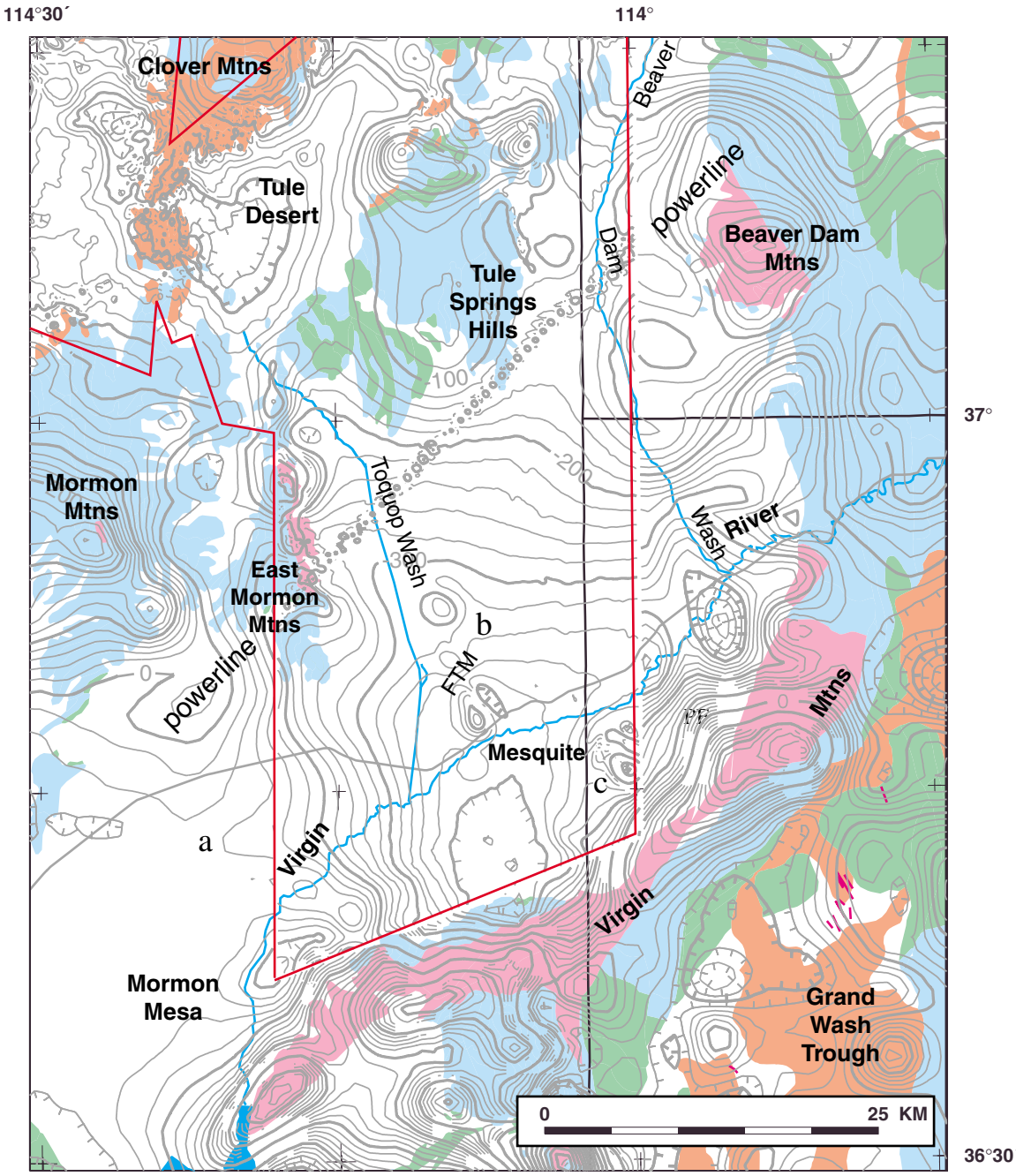


Figure 5a. Aeromagnetic contours on simplified geology. Contour interval, 20 nT. See figure 2 for explanation of geology. "a", "b", and "c" refer to anomalies discussed in the text.

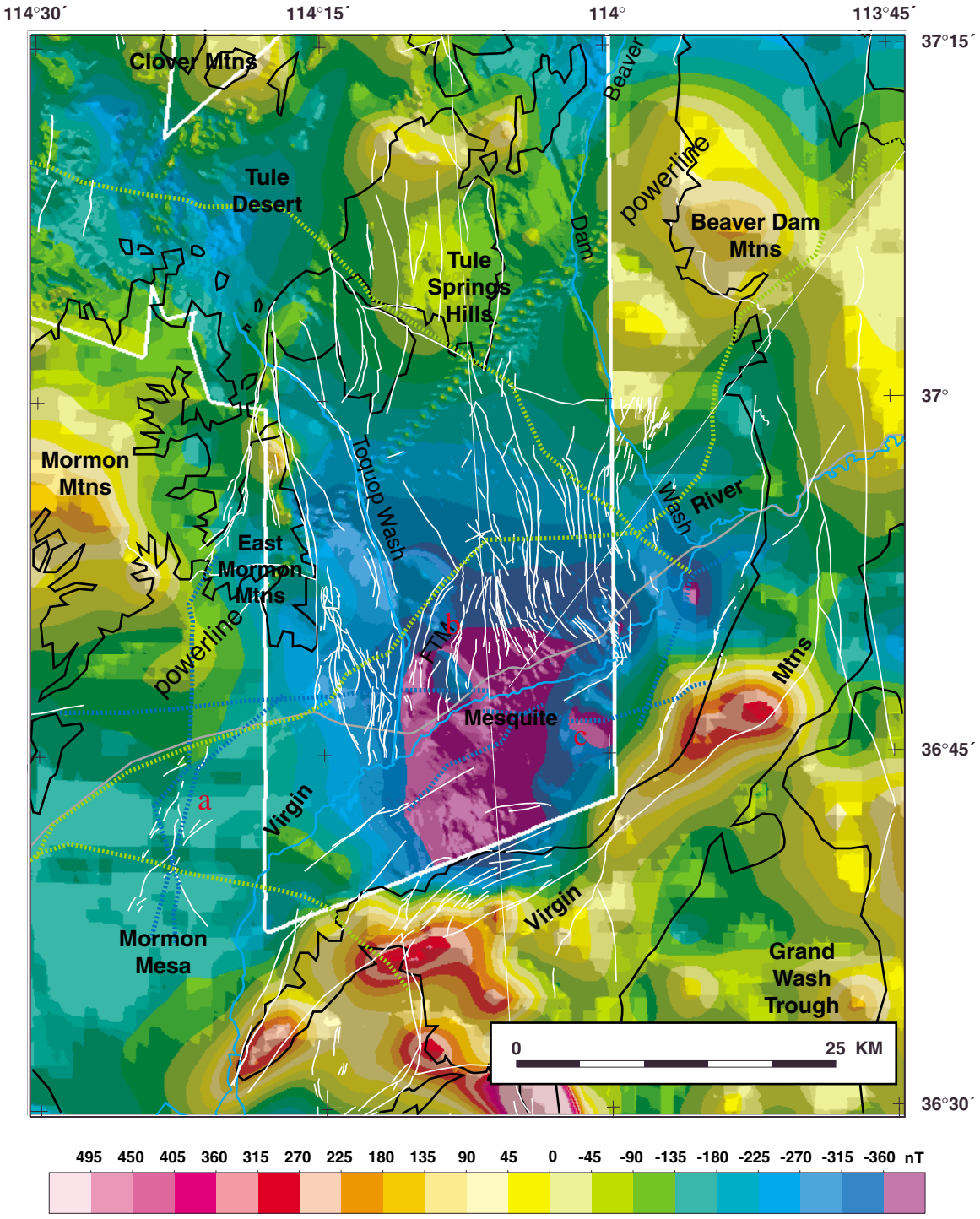


Figure 5b. Color shaded-relief magnetic map of the study area. Contour interval, 45 nT. Solid white lines are mapped faults. Dotted green and blue lines are seismic-reflection profiles from Carpenter and Carpenter (1994) and Bohannon and others (1993), respectively. Black lines show extent of pre-Cenozoic basement.

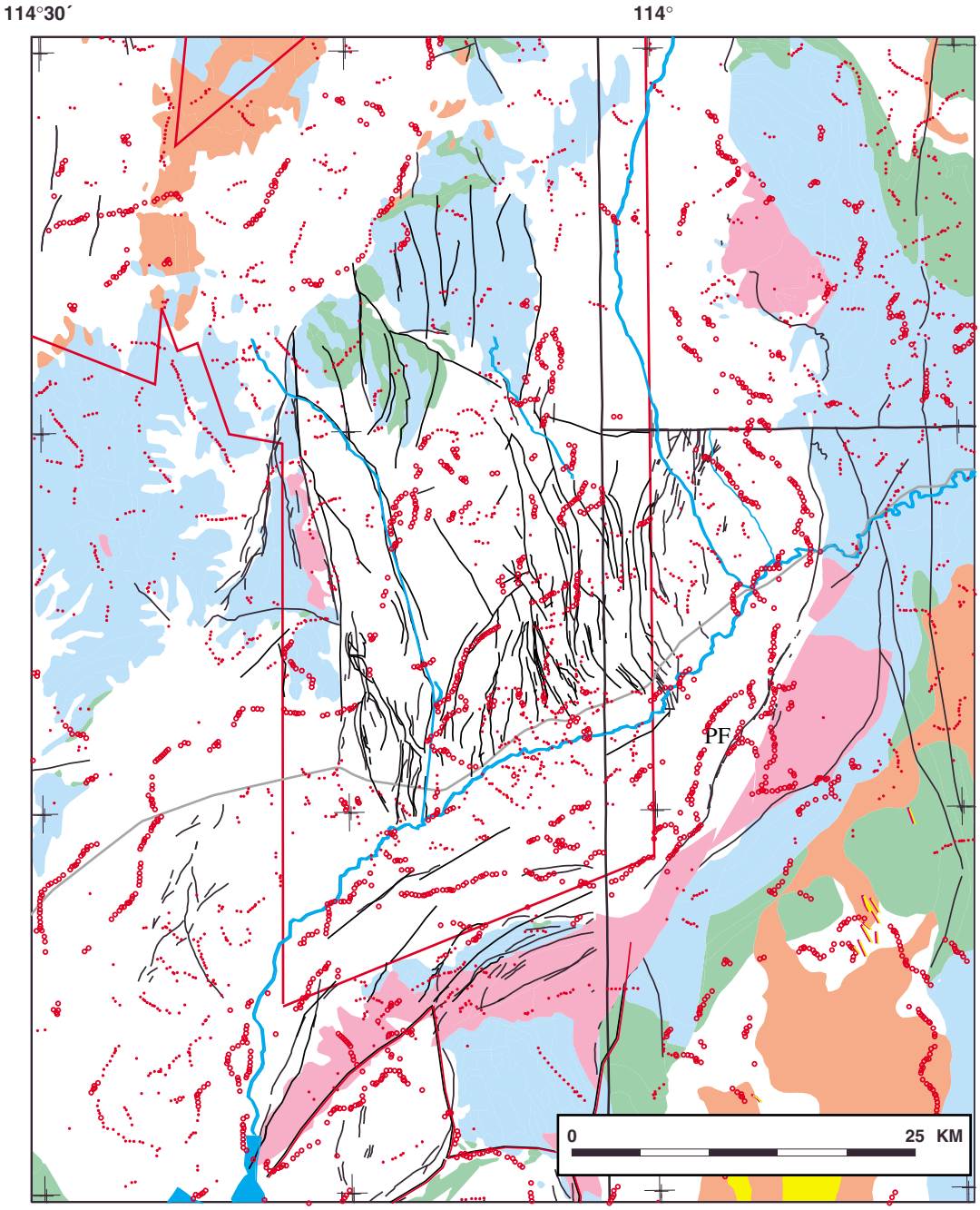


Figure 6a. Density boundaries (red circles) plotted on simplified geologic map. See figure 2 for explanation of geology.


Figure 6b. Magnetization boundaries (in black plotted on filtered aeromagnetic data to enhance shallow sources. Red lines, faults; gray lines, extent of pre-Cenozoic basement.

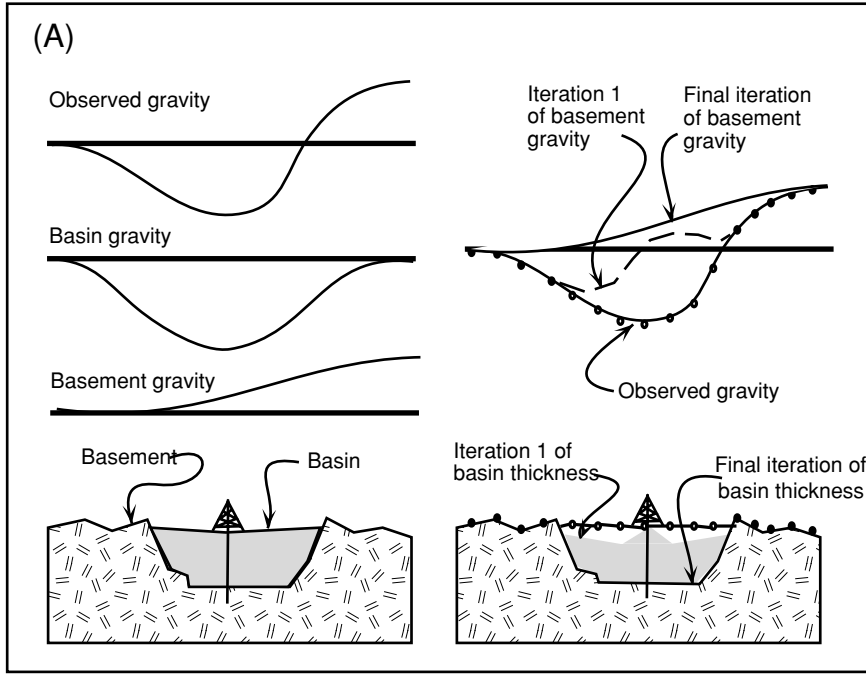


Figure 7 Schematic representation of the gravity separation procedure.

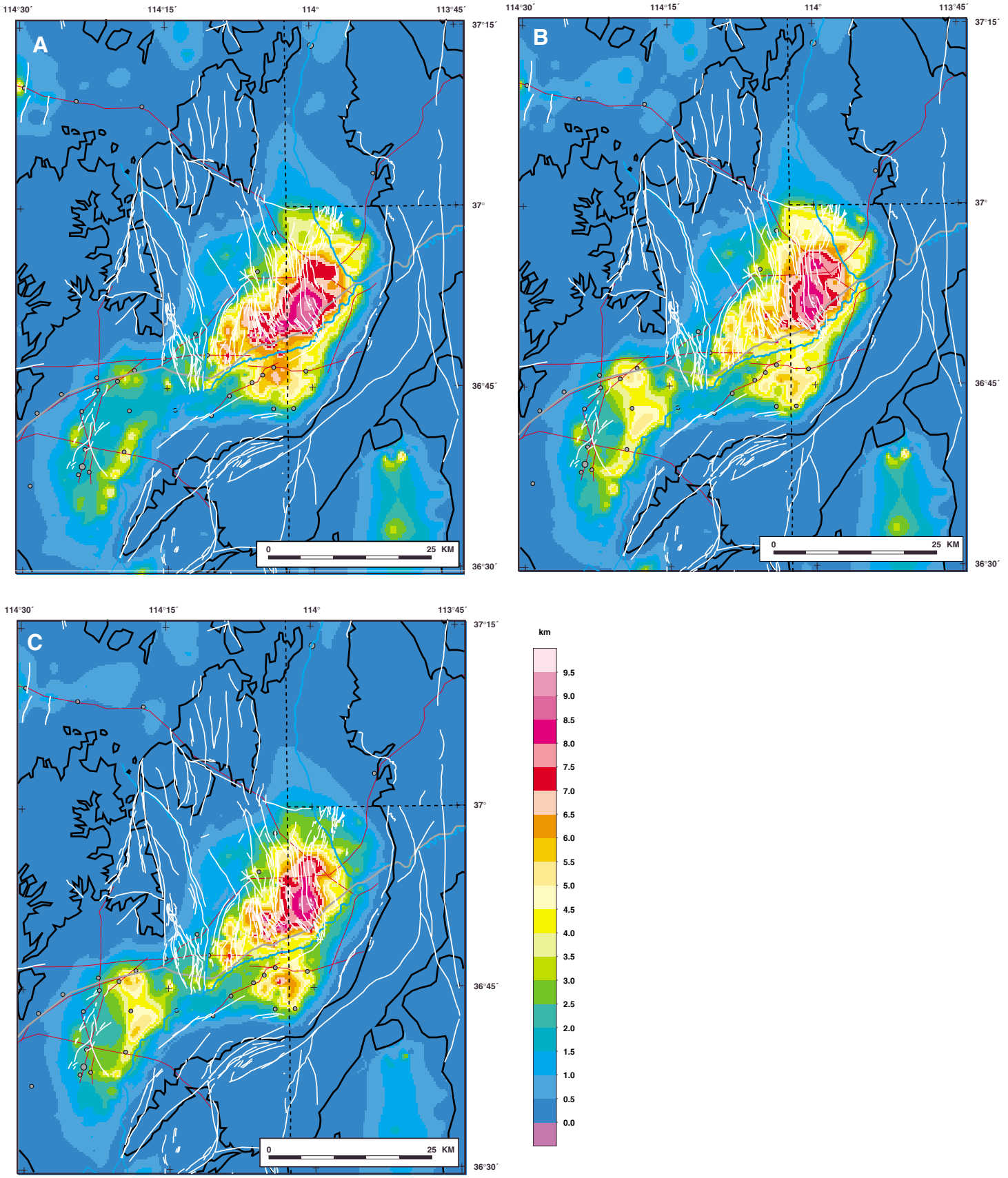


Figure 8. Basin thickness models. (A) Using density-depth function derived from Virgin Mobil 1A and only basement gravity stations. (B) Same density-depth function, but including well and seismic data. (C) Density-depth function derived from Carpenter and Carpenter (1994) and all well and seismic data. Contour interval, 500 m; well and seismic picks in gray and black circles. Faults shown in white. Seismic lines in red.

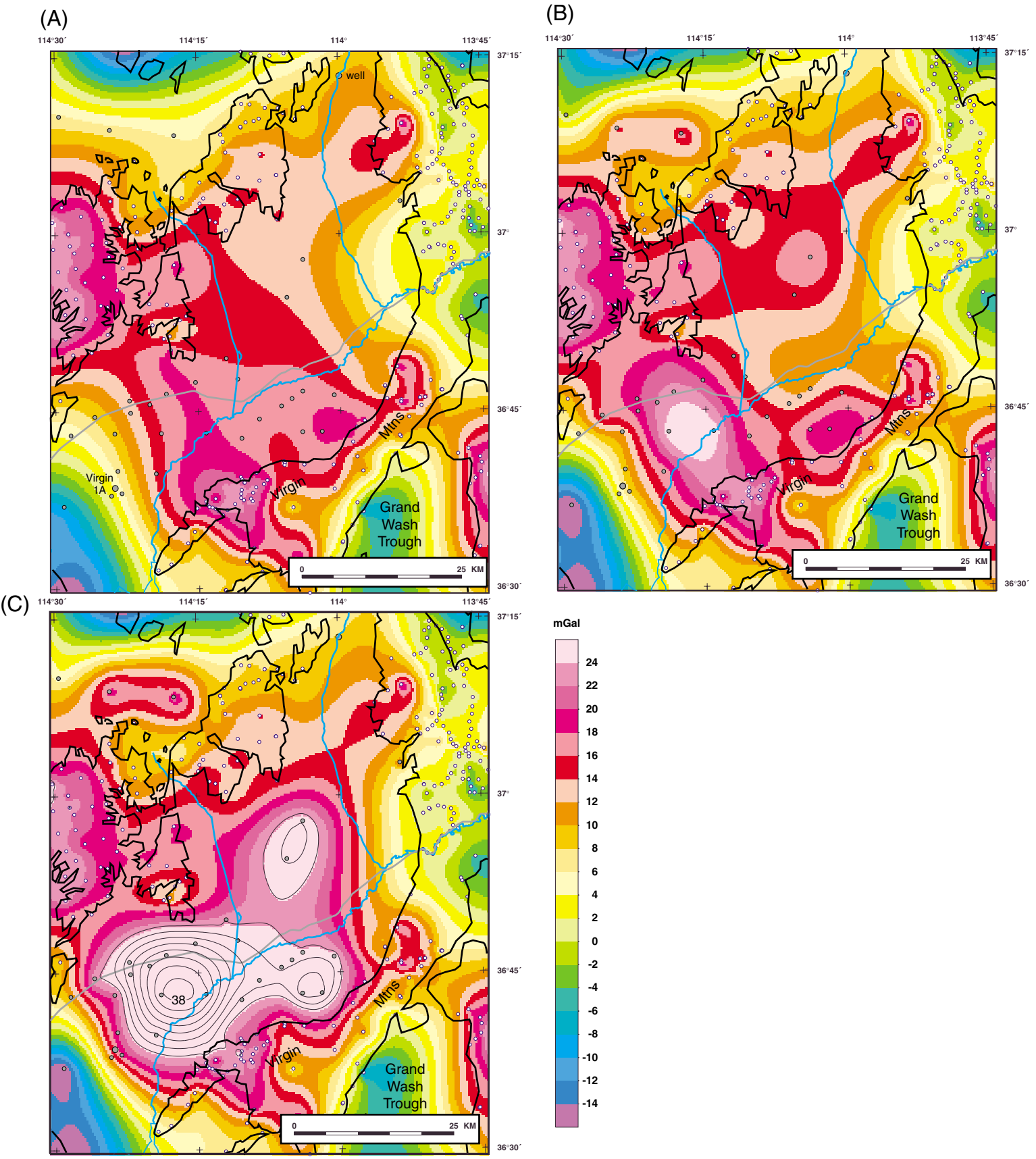


Figure 9. Basement gravity. Contour interval, 2 mGal. Basement gravity stations, white and black circles; well and seismic picks, gray and white circles. (A) Density-depth function from Mobil Virgin 1A and using only basement gravity stations. (B) Same density-depth function, but using wells and seismic picks in addition to basement gravity stations. (C) Density-depth function derived from Carpenter and Carpenter (1994) and using wells, seismic picks, and basement gravity stations. Maximum basement gravity value, 38 mGal in (C).

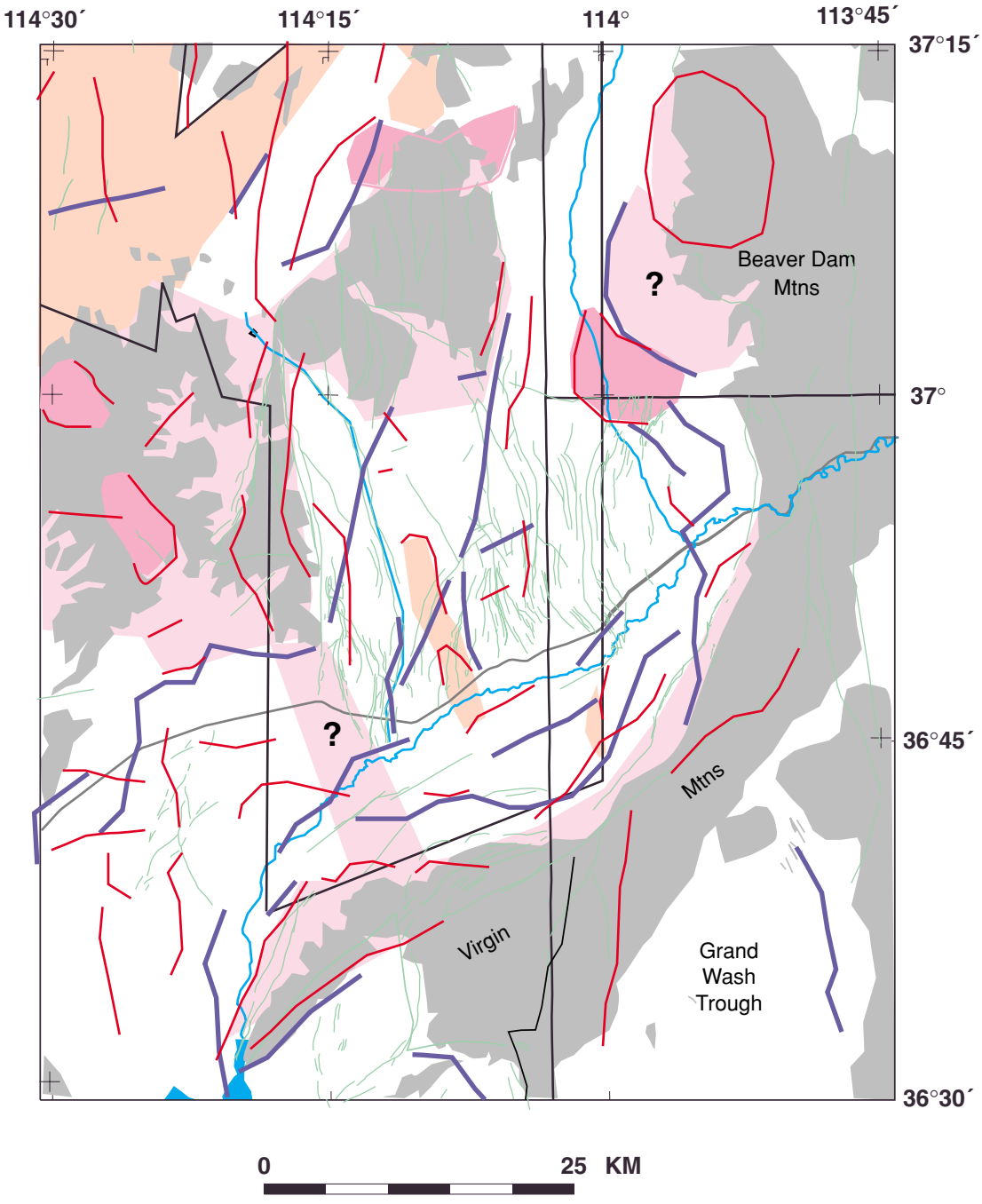


Figure 10. Structural framework derived from geophysical data. Boundaries derived from gravity and magnetic data, shown in dark blue and red, respectively. Mapped faults shown in light green. Gray, extent of pre-Cenozoic basement exposures. Pink, shallow (< 4 km) Precambrian basement. Dark pink, shallow Tertiary intrusion or Precambrian basement. Orange, shallow Tertiary volcanic rocks.

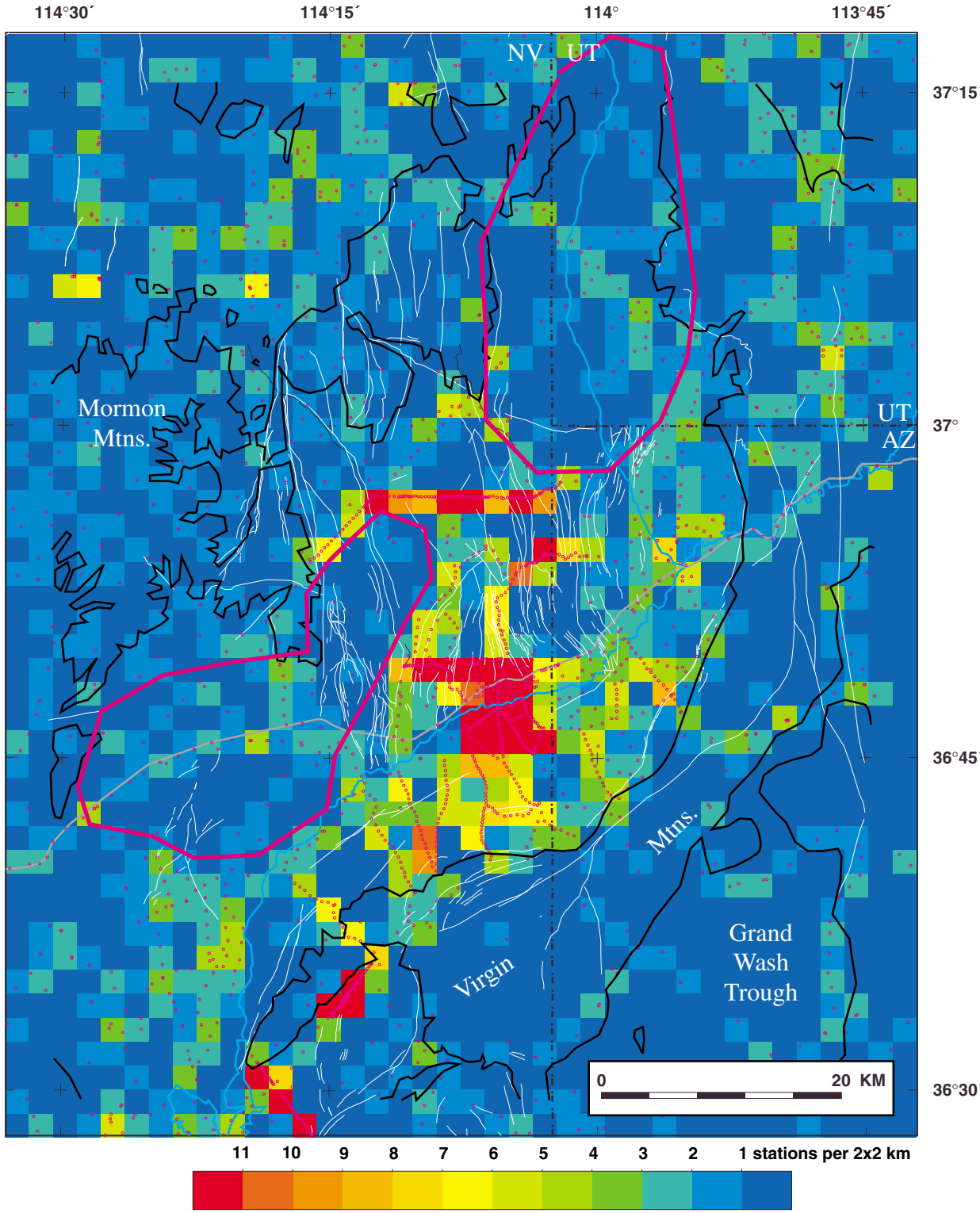


Figure 11. Map showing number of stations per 4 km$^2$ area. White lines, faults. Gravity stations shown as magenta crosses. Magenta lines outline areas of sparse gravity stations in areas of potential hydrologic interest. The Mormon and Virgin Mountains and Grand Wash trough are also characterized by poor station coverage. Black lines show extent of pre-Cenozoic basement.